

**Thin deformable mirrors for a reconfigurable space
telescope**

Journal:	<i>53rd AIAA/ASME/ASCE/AHS/ASC Structures, Structural Dynamics, and Materials Conference</i>
Manuscript ID:	1220023
luMeetingID:	2414
Date Submitted by the Author:	02-Apr-2012
Contact Author:	Patterson, Keith

SCHOLARONE™
Manuscripts

Thin Deformable Mirrors for a Reconfigurable Space Aperture

Keith Patterson* Namiko Yamamoto[†] and Sergio Pellegrino[‡]

California Institute of Technology, Pasadena, CA 91125

As part of a small satellite technology demonstration mission that will utilize autonomous assembly, reconfiguration, and docking technology to form the primary mirror for the mission's telescope payload, the mirror segments are required to modify and control their shape, in order to allow for imaging in different configurations. This paper focuses on the development of 10 cm diameter active lightweight mirrors. The current mirror design, control scheme, and fabrication methods are described, as well as experimental results on initial samples. The data demonstrates that the mirrors are capable of at least 100 microns of displacement during operation, and that fabrication on polished molds can result in high quality reflective surfaces.

I. Introduction and Background

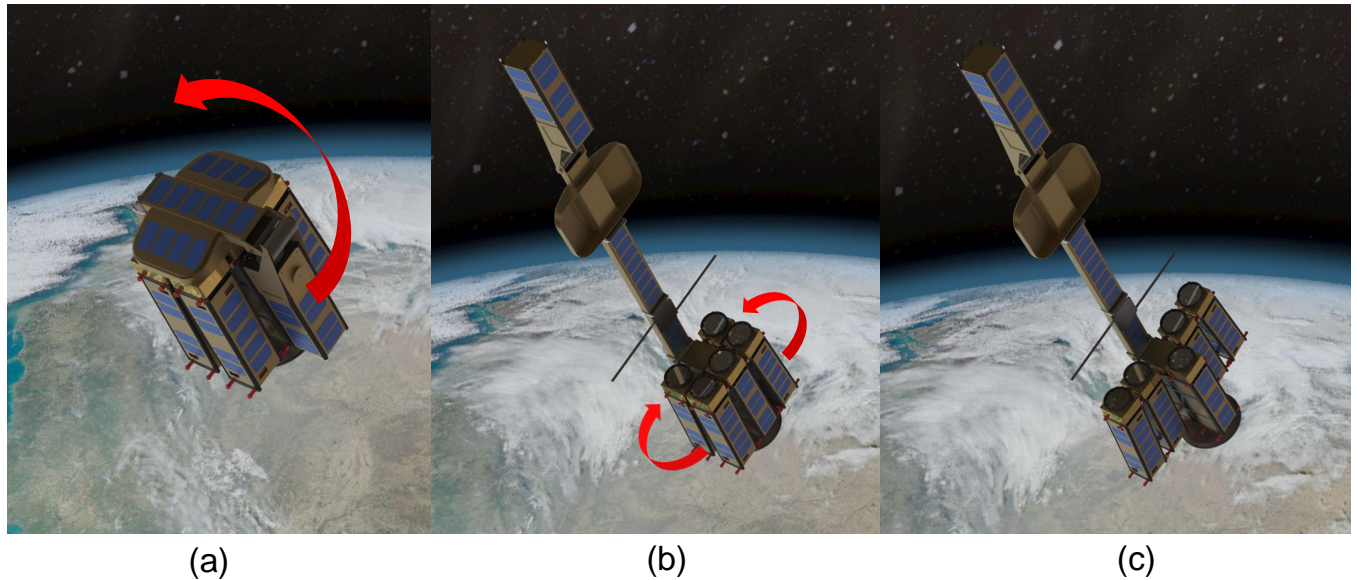


Figure 1. Concept illustration for a technology demonstration mission for the on-orbit assembly of a space telescope. The Cubesat-based telescope launches in a stowed configuration (a), deploys its detector package (b), and autonomously reconfigures its aperture (c).

Space-based telescopes have been constrained by the size of available launch vehicles but this limitation may finally be removed with the launch of the first folding primary mirror in the James Webb Space Telescope,

*Graduate Student, Graduate Aerospace Laboratories, 1200 E. California Blvd. MC 205-45. kdpatter@caltech.edu

[†]Postdoctoral Fellow, Keck Institute for Space Studies, Graduate Aerospace Laboratories, 1200 E. California Blvd. MC 205-45. namikoy@caltech.edu

[‡]Joyce and Kent Kresa Professor of Aeronautics and Professor of Civil Engineering, Graduate Aerospace Laboratories, 1200 E. California Blvd. MC 301-46. AIAA Fellow. sergiop@caltech.edu

currently under construction. This is a major step forward in space telescope technology, however the cost and complexity associated with folding mirror architectures and the size limitations still inherent in this approach will ultimately necessitate even more radical approaches. Considering the time it takes for a new space observatory concept to reach maturity, the search for such alternatives should begin now.

We have participated in a study of large space apertures sponsored by the Keck Institute of Space Studies (KISS).¹ This study put forward the concept of forming a large mosaic mirror through on-orbit self-assembly of relatively small mirror segments mounted on separate low-cost spacecraft, building on recent developments in autonomous self-assembly in space.²⁻⁵ The spacecraft would dock and become mechanically connected and the mirrors would adjust their shape to form a single coherent mirror surface. As a follow-on to this study, we have been studying the feasibility of a low-cost technology for lightweight mirrors to be used on each of these spacecraft.

A concept for a precursor mission has been developed in order to demonstrate, on orbit, the new technologies needed for this radical architecture. This mission would demonstrate, using small nanosatellites, the autonomous assembly and docking of telescope components, as well as lightweight active mirrors.

In this paper we present an overview of the demonstration mission and the role of thin, deformable mirrors in this mission, as well as the predicted performance of the mirrors. The mirrors have an active laminate construction with various actuation patterns embedded directly into the film, allowing for a flexible, lightweight mirror with large actuation capability. The bulk of the paper focuses on the concept, design, and manufacturing process for these mirrors. Results of initial testing on mirror samples are presented, and the paper is summarily concluded with an outlook on future development work.

The paper is organized as follows: Section II describes the mission concept, Section III describes the mirror concept, Section IV discusses the current mirror design in more depth, Section V gives a brief description of the fabrication steps, Section VI gives the testing results, and Section VII concludes the paper.

II. Overview of Demonstration Mission and Telescope Concept

Our latest demonstration telescope concept is shown in Figure 1. The telescope is a prime focus design (1.2 m focal length, 1.0° field-of-view) with the primary mirror divided up into a sparse aperture consisting of an arrangement of 10 cm diameter circular mirrors. The primary mirror segments are attached to a cluster of Cubesats (mirrorsats), two of which are able to undock from the cluster and navigate independently. The telescope would launch as a small secondary payload in a stowed state as seen in Figure 1 (left). The stowed volume of the telescope is 0.5m by 0.5 m by 0.6 m. After separation from the primary payload, the telescope would deploy its sensor package to the focus of the mirror array using a hinged mast.

The sensor package contents include a detector at the image plane, corrective lenses to compensate for the prime focus design, as well as a Shack-Hartmann wavefront sensor. Using the wavefront sensor within the camera package for mirror shape information, the mirrors would be adjusted and calibrated in order to minimize the size of the mirrors' individual point spread functions (PSF). The mirrors would not be co-phased down to sub-wavelength levels (as would be required for a proper science mission), as this would require an additional metrology system that is prohibitively expensive for a small mission like this. Instead, images would be taken to demonstrate the ability of the mirrors to self-correct their shape, as well as the ability to re-point and correct the individual PSF's.

When the initial calibration and imaging demonstration is completed, two of the mirror segments, which are carried by independent Cubesats equipped with propulsion systems, would detach from the mirror cluster, perform a maneuver to reposition themselves at a new location in the array, and then redock to the cluster (Figure 1 (right)). This would demonstrate on-orbit assembly of the mirror segments.

Once the cluster is again assembled, the mirror calibration and imaging would be performed again to show the capability of calibration in various configurations. To be successful, the new array positions of the mirrors would require them to be adjustable in order to achieve focused PSF's. To achieve diffraction-limited PSF's, the mirrors surface accuracy must be controlled down to the order of fractions of the telescope's observational wavelength. For the visible band, this requirement is on the order of tens of nanometers. Hence, the mirrors have to be able to provide relatively large shape changes, or stroke, between different configurations which is on the order of microns, with an accuracy on the level of tens of nanometers. Figure 2 quantifies the required deflections for the mirrors in different array position from a reference (or "OFF") shape assumed to be common to all mirror segments. These plots result from an assumed reference shape that is spherical, such that the required deflections of the mirrors is minimized.

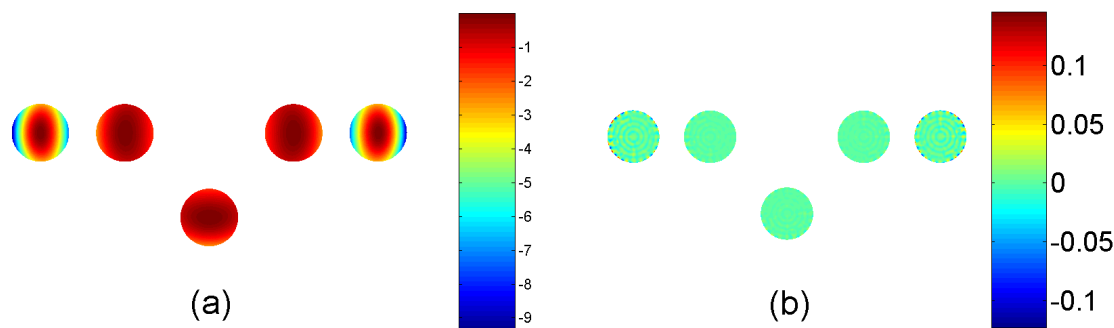


Figure 2. Required mirror deflections (in units of waves, 633 nm) across the various mirrors in the telescope aperture prior to calibration (a). Calculated remaining errors (also in waves) after mirror adjustments (b). The RMS error is 5.1 waves before correction, and 0.02 waves afterwards.

III. Mirror Concept

Reducing the mass of large space telescopes is critical. In keeping with this design philosophy, the deformable mirrors of the telescope will be designed to be thin and light-weight. The actuation of the mirrors will be accomplished by in-plane, or surface parallel, actuation through the use of piezoelectric materials rather than using externally applied loads to deform the mirror, which would require a backing structure. In order to stabilize the nearly flat, low stiffness thin mirror, a semi-rigid ring will encircle the mirror, to which the mirror will be attached. In order to retain complete actuation authority over the mirror surface, this rim will also be active through the use of piezoelectric actuators. At small scale, the mass of the rim is larger than the mirror film itself, however, if these mirrors are scaled to larger sizes, the mass of the rim scales only linearly, while the impact of the quadratic scaling of the film mass is alleviated by its small thickness.

Surface parallel actuation necessitates the lamination of active materials to the mirror surface. To provide a broad family of allowable shape adjustments, the active materials are divided up into various individually addressable regions. Several possible patterns of actuators on a representative mirror model are shown in Figure 3. The plots show the distribution of shape adjustment due to one of the actuators being activated. This mode shape is known as the actuator's influence function.

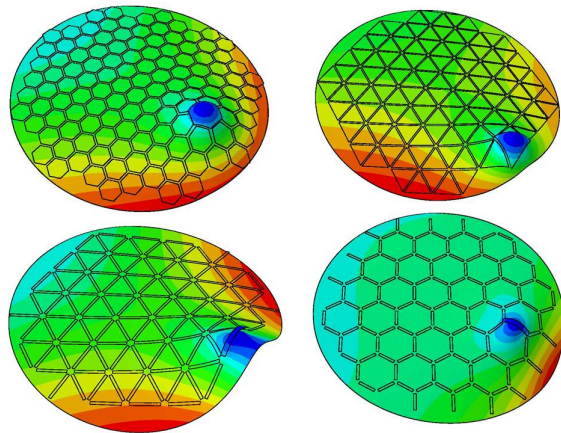


Figure 3. Comparison of influence functions of different actuator patterns.

IV. Mirror Design

This section presents a broad description of the design established thus far for the 10 cm diameter deformable mirrors. This includes the materials used for the mirror film, the layout of the laminate layer within the mirror, electronic control scheme, as well as the mounting concept.

A. Material Selection

The primary material used in the mirror construction is polyvinylidene fluouride, PVDF, or its co-polymer poly(vinylidene fluouride trifluoroethylene), P(VDF-TrFE). These materials are semi-crystalline electro-active fluoropolymers which can be made piezoelectric with proper processing. While PVDF has a stronger piezoelectric coefficient, it must be stretched or specially processed in order to align the polymer chains and attain the proper piezoelectric crystal phase. The copolymer has a weaker piezoelectric effect, but it does not require stretching, and therefore does not suffer from the associated in-plane anisotropy in its properties that are caused by this process.

An extensive study has been done by Sandia National Labs²² on the performance of PVDF under LEO-like conditions including temperature range, UV exposure, atomic oxygen, and other effects. While there are restrictions on allowable temperatures on the material (approx. -80°C to 90°C) to prevent loss of piezoelectric properties, and there is some degradation of the film by atomic oxygen, the overall conclusion of the study was fairly optimistic on the prospects of the use of the polymer in space. During this study some samples were sent to the International Space Station, but an analysis of the returned samples has yet to be completed.

Some concerns that remain with the use of PVDF for space mirrors include the necessity of a proper thermal design to prevent the material from being exposed to extreme temperatures, the thermal stability of the material, passive charging of the material in the space plasma environment, as well as creep and relaxation of the material under applied stress and/or electric field (e.g. see Figure 4). It is the authors' belief that proper design of the mirror controller, shape sensing scheme, and thermal control can alleviate these concerns and allow the material to be used for mirrors in LEO.

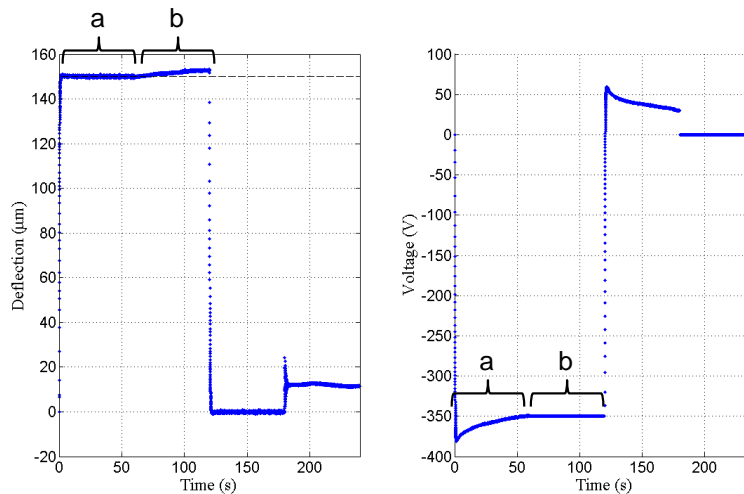


Figure 4. Creep relaxation behavior of a PVDF bimorph beam under (a) constant deflection or (b) constant voltage conditions.

B. Electrode Patterns

In order to actuate the piezoelectric material, it must be coated on both sides by metal electrodes, and an electric field placed through the material to produce the desired piezoelectric response. In order to provide greater control over the range of achievable shapes as well as robustness, the electrodes should be divided up into individual regions that allow for independent control of various regions of the material. In previous work,¹⁶ comparisons between several basic electrode patterns were performed in order to determine which pattern provides the best capability for reducing residual errors in a specific application. A plot showing a

comparison of actuator-induced deformations is shown in Figure 3. The pattern density was also varied in order to determine the minimum number of actuator channels required to achieve an adequate performance.

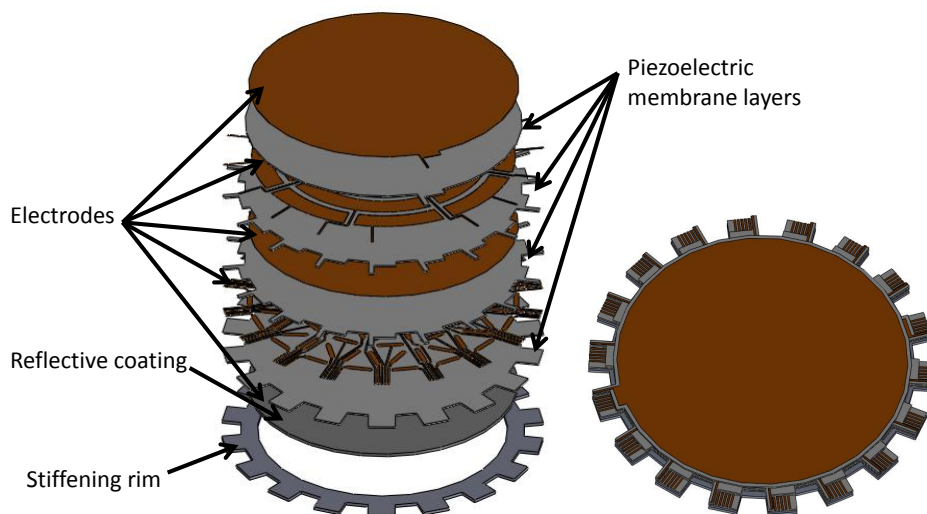


Figure 5. Exploded view of layers forming the mirror film stack.

A combination of a fine triangular lattice pattern together with a coarse annular pattern (see Figure 5) was chosen for the initial mirror design. The coarse annular pattern is added to aid changes in mirror focal length (overall mirror curvature) without using up the available stroke of the fine pattern electrodes. The triangular lattice would be used to fine-tune the shape once the mirror approaches the optimum curvature. In order to allow for two different patterns with the required associated ground layers, it is necessary to expand the number of piezo layers to four, with five electrode layers interlaced, including the mirror reflective layer which would also be used as an electrode. In total there are 106 actuators in this design, 90 from the fine pattern, and 16 from the coarse pattern.

Using a finite element model developed in the Abaqus CAE software, it was possible to simulate the corrective capability of a mirror with such a design. The mirror was modeled as a composite laminate with S3T/S4T thermo-elastic shell elements. Linear piezoelectric strains were introduced using appropriately scaled thermal expansion in the software. For small displacements about the initial shape, a linear analysis was performed assuming that the influence function from each actuator can be combined in a linear fashion to produce the deformed shape. This analysis was similar to previous work.^{16,17}

The results for the current mirror design are summarized in Figure 6. The horizontal axis displays the first few Zernike modes of deformation for the circular mirror. The blue curve depicts the capability of the mirror to correct each particular mode, with its corresponding scale on the left. For example, an error in focus (the first mode shown) can be corrected by a factor of 200x the original error magnitude. The capability of the mirror to fix errors in each mode decreases and the mode order (or spatial frequency) increases as expected due to the finite number of actuators. The green curve depicts the maximum stroke for each mode and its scale is on the right side in units of waves (633 nm for this study). The linear model predicts that the focus mode can be changed by almost 1000 waves (about 0.6 millimeters), although this number is an overestimate because inclusion of nonlinearities introduced by the mirror's in-plane stiffness, which would begin to act against the deflection as the magnitude becomes relatively large, were not included in this model.

C. Controller

The mirror controller is based partly on a design proposed by Song et al.²¹ It consists of a microcontroller whose analog output is amplified to the -500 V to +500 V range by a single high voltage amplifier, and then multiplexed into the individual capacitive actuator channels. The controller cycles through each actuator and sets the channel voltage. The voltage level is then held with some minor leakage until the next refresh cycle. This allows control over a large number of actuators from a single controller board and amplifier

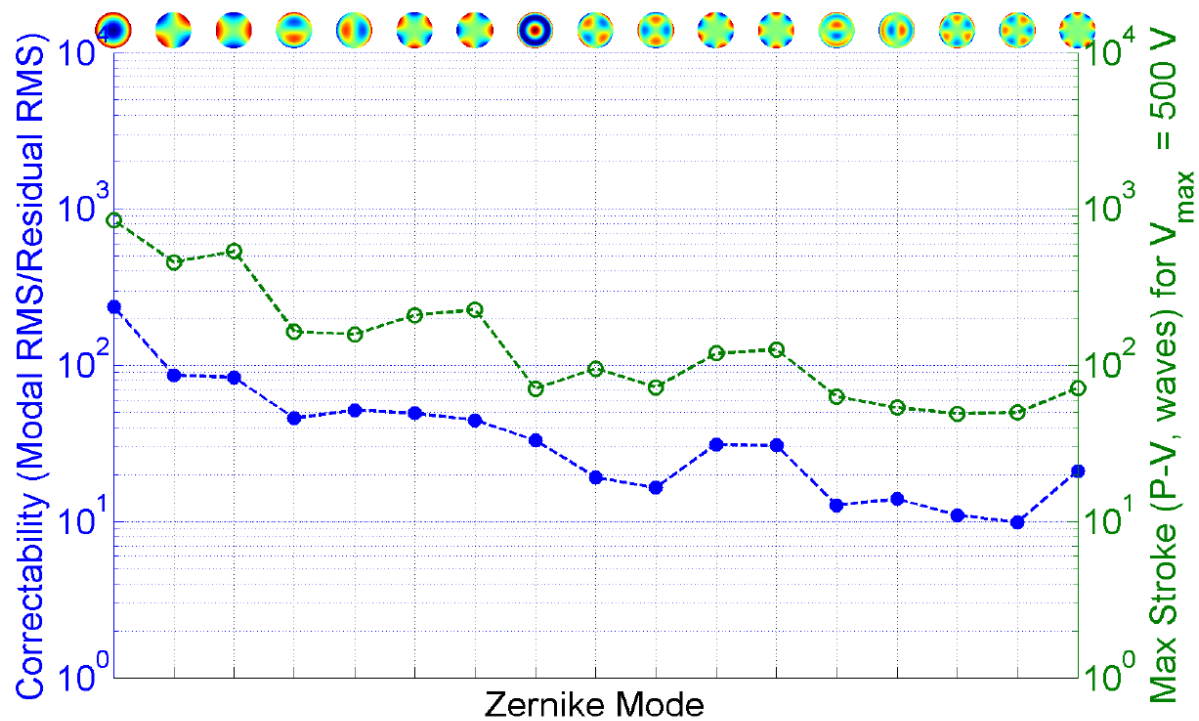


Figure 6. Predicted capability of 10 cm mirror across the various Zernike deformation modes. Modeling was done using Abaqus CAE.

board at the expense of control frequency bandwidth. The general concept schematic is shown in Figure 7, and the multiplexing concept is illustrated in Figure 8. This design is ideal for accounting for most low frequency disturbances (thermal, viscoelastic creep, etc.) that can be expected in the space environment. For high frequency disturbances (e.g. momentum wheel vibrations), additional dedicated controllers could potentially be added to a limited number of channels to actively dampen the disturbance.

D. Mounting

Mounting is a critical component of the mirror design. A thin shell structure is not stable without a stiff edge frame. The simplest rim is a ring attached to the edge of the mirror film. The frame should be outfitted with actuators to provide an adjustable boundary condition for the mirror. For example, the rim should be able to expand or contract in order to accommodate bulk thermal motion of the mirror laminate. It should also be able to deform out of plane so as to adapt to the outer profile of the desired optical surface.

The mounting rim also needs to provide an electrical interface to the film. Electrodes within the mirror laminate have traces that run from the mirror interior to metal pads on the edge as seen in Figure 5. These pads then lie over the supporting surface of the rim, where wire bonding or other techniques can be used to connect wires for each channel.

The mirror along with the rim is then stable enough to be attached kinematically on a gimbaled mount for bulk rigid body positioning and pointing of the mirror. For the demonstration mission, this mount will only provide three degrees of freedom: piston, tip, and tilt. The other three motions can be accounted for by slightly changing the desired prescription of the mirror.

V. Fabrication

PVDF and its copolymer are thermoplastic materials that are soluble in certain organic solvents. By spreading a viscous liquid solution of the polymer over the surface of a polished mold, and then allowing the solution to dry, a thin film of PVDF can be produced. This process can be repeated to produce thicker

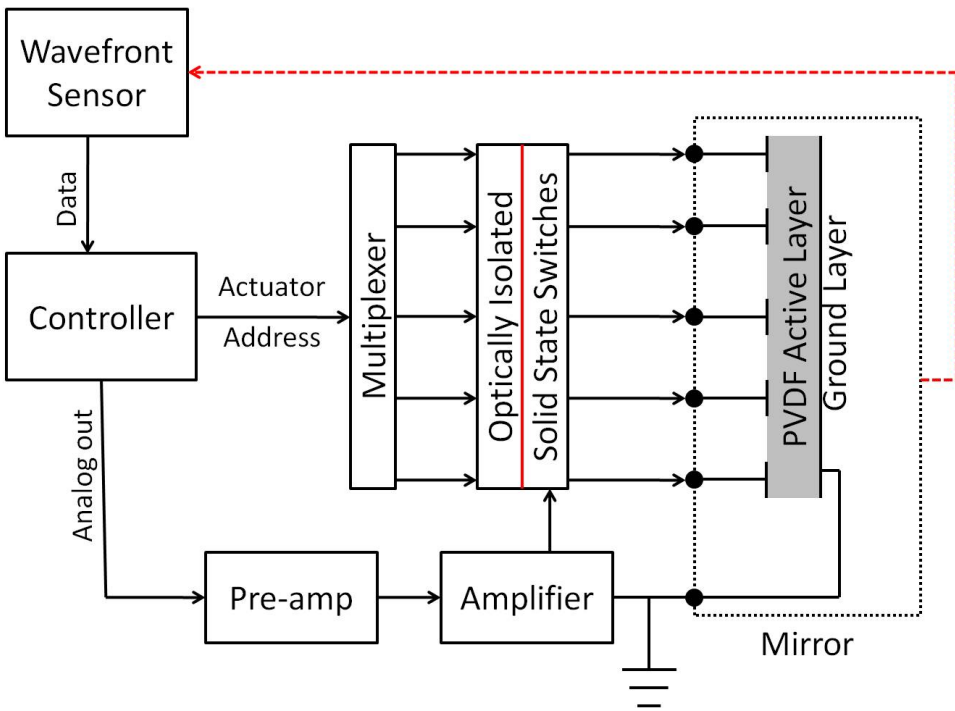


Figure 7. Flowchart showing closed loop mirror control.

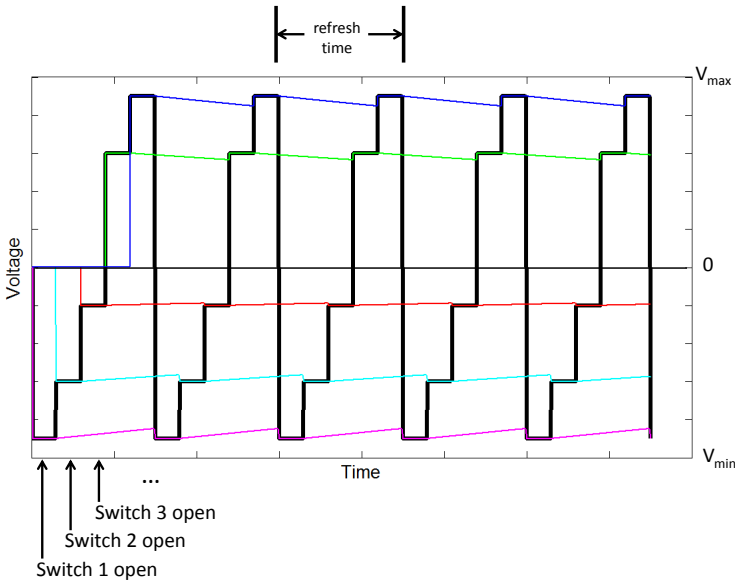


Figure 8. Traces showing time-varying high voltage input (heavy, black) and multiple actuator channels (light, colored) that shows a steady quasi-DC level. Channel decay between refresh points is exaggerated for illustration.

films. The preferred method of application of the solution is to use the spin coating technique, which is common to microelectronics fabrication. By adjusting the spin speed and duration the thickness of the film can be controlled.

For samples that have been made up to this point, we have used polished Silicon wafers as molds. Starting from a fresh wafer, a thin layer of polyimide is applied as a base layer also using spin coating. The polyimide layer will later support the reflective mirror coating, and the material produces a very good surface finish after high temperature curing. As a commonly used material used in microelectronics fabrication, there are also readily available chemicals and processes that can improve or reduce adhesion of polyimide to the wafer, as desired, depending on the chosen method for releasing the mirror from the wafer.

After the base layer is applied, layers of the piezoelectric polymer are alternated with metal patterns that are deposited via physical evaporation or sputtering methods. Deposition occurs through a physical shadow mask that blocks deposition in regions where no metal is desired.

Depending on the nature of the deposition material, electrode material used, and CTE mismatches, large stresses may develop in the thin metal films. It is important to carefully control the process to reduce stresses and promote good interlayer adhesion so as to prevent the development of cracks and defects in the electrode and/or polymer layers. The usage of high voltage during the poling process necessitates a high dielectric strength of the polymers, and defects can substantially reduce this strength and cause electrical breakdown failures.

Once all of the layers have been deposited, several methods to separate the mirror film stack from the Silicon wafer have been identified. The simplest method is to simply ensure low adhesion between the base layer and the wafer, and to peel to the film away. However, this can lead to damage of the film, as well as causing stress during the delamination process. Also, low adhesion to the Silicon sometimes causes problems during later processing of the upper layers. Another method is to put down a layer between the mold and base layer which acts as a release layer when dissolved in a solvent. However, due to the sensitivity of the polymer layers to most solvents, this is not a very attractive option.

A more elegant, yet time consuming method is to etch away the wafer itself. This can be done through the Deep Reactive-Ion Etching (DRIE) process from the underside of the wafer. Some material may be left as a rim if a DRIE resistant patterned silicon oxide coating is applied to the wafer underside. A rim is attractive since its stiffness stabilizes the film, and prevents it from curling or rolling up due to any residual internal stresses. A small amount of residual tension left remaining in the mirror film contributes to maintaining the film flat, see Figure 9.

VI. Testing

Initial testing of mirror samples has been carried out. Starting from simple unpatterned samples in order to confirm the poling process, material properties, and general behavior. The mirror laminate was bonded to a dummy rim and separated from the mold. The rim holds a constant shape and does not accommodate the laminates shape changes. The out-of-plane deflection of the central point of the mirror was measured while varying the voltage to the mirror electrodes. All tests were performed at room temperature.

1. *Single Actuator Mirrors*

The simplest samples tested were layers of 25 μm thick P(VDF-TrFE) coated on two sides with continuous blanket layers of thin metallization. The rim is 80 mm in diameter. The samples initially started with a flat surface due to residual tension in the film upon separation from the silicon substrate.

Upon application of a low frequency sinusoidal voltage to the virgin mirror material, the response was quite small with a quadratic dependency on the voltage. This response precluded motion in two directions and moved only in a single direction regardless of the electric field direction. Figure 11 shows a plot of an example response. The type of behavior is indicative of electrostrictive materials or even simple dielectric elastomers reacting to the compressive stress applied by the attraction of two oppositely charged parallel plates (Maxwell stress), by having an in-plane expansion (Poisson's effect).

As the material was cycled through larger and larger voltage amplitudes, see Figure 12, the semi-crystalline material began to align its domains with the applied field, causing increasing amount of hysteresis. This continued to develop into a skewed analogue of the classic piezoelectric butterfly curve. The electric field level required to cause this transition from unpoled to poled is referred to as the coercive field.



Figure 9. Film sample attached to a rim, showing the quality of the reflective front surface that can be achieved by replication from the wafer mold. Damage caused by peeling of the film stack from the silicon wafer can be seen around the edge.

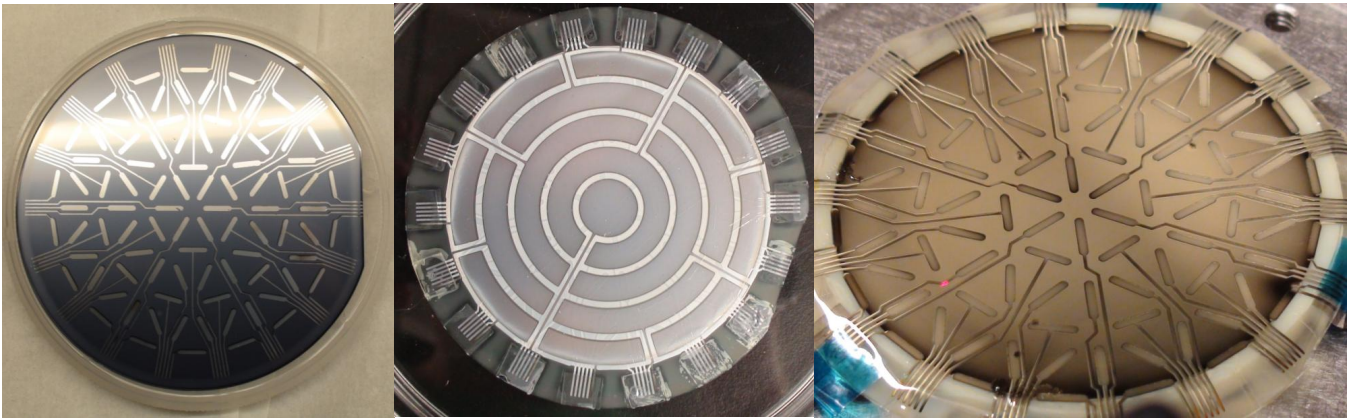


Figure 10. Photos of samples showing the fine pattern (left), coarse pattern (center), as well as a freestanding completed stack sample after separation from the mold (right).

For these samples, the coercive voltage was about 2000 volts, corresponding to an electric field strength of approximately $80 \text{ V}/\mu\text{m}$. When the field returned towards zero, it can be seen that the response became quite linear. Figure 13 shows 10 cycles in the planned operating regime of -500 to 500 volts after the poling process. The response was very close to linear with very slight hysteresis. There was a slight remaining curvature that is likely due to residual electrostrictive or dielectric behavior. Note that the noise and drift of the Keyence LK-G157 laser measurement was on the order of 5 to 10 microns even with the voltage off, which is close to the magnitude of the non-repeatability in the measurement. It is therefore possible that the hysteresis is even smaller than implied by Figure 13.

The magnitude of the response is over 100 microns within the operating voltage range, which is rather large for a deformable mirror of this size. However, there is a large residual deformation that is left by the hysteresis of the poling process. The fabrication process of the mirror film needs to be adjusted in order to accommodate the associated strains of poling.

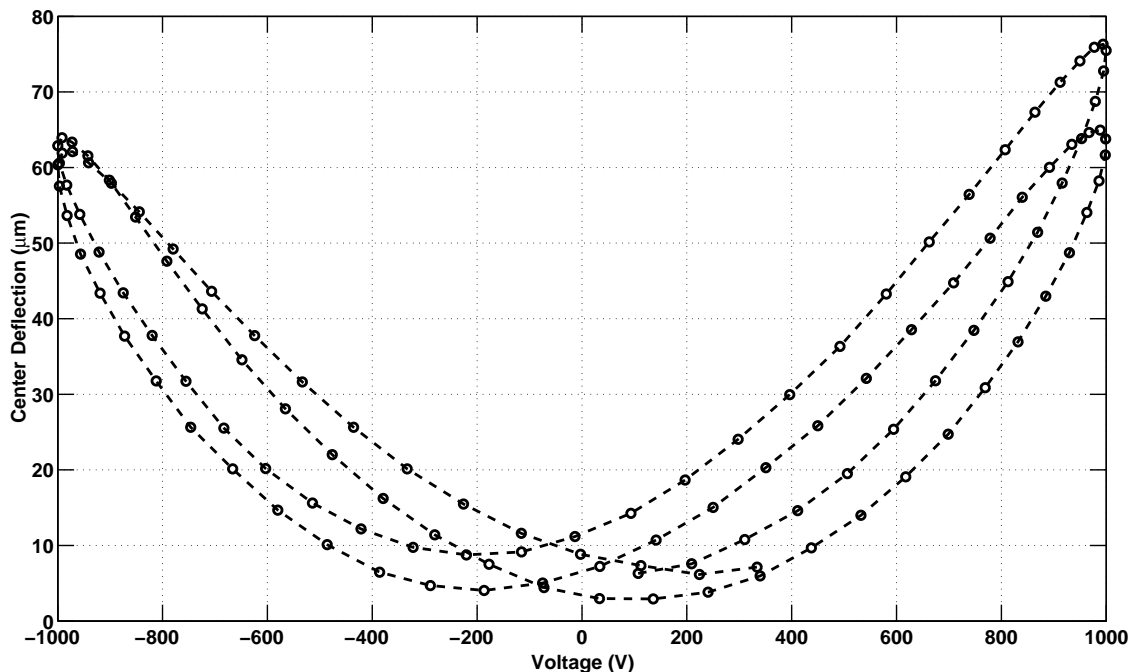


Figure 11. Deflection of the center point of a single-actuator mirror sample prior to poling of the material. The observed behavior is indicative of a weak electrostrictive or dielectric elastomeric response.

2. Multi-Channel Mirrors

Mirror samples have been built incorporating all of the designed layers and electrode pattern. An example can be seen on the right side in Figure 10. Work is currently ongoing in order to implement a mounting and connection scheme in order to interface with these samples.

VII. Conclusions

The concept and fabrication process have been established for a new type of deformable mirror. The fabrication methods to build the mirror film have allowed us to produce smooth mirror surfaces using silicon wafers, and work will continue on improving the quality of the mirrors. Initial testing has been performed on single actuator samples, and additional testing will be performed on multi-actuator mirrors shortly once the mounting scheme has been established. These multi-channel mirrors will be installed into an optical testbed that includes a Shack-Hartmann device to enable closed loop control of the mirrors. Significant challenges remain to be overcome in order to demonstrate shape control down to optical quality levels.

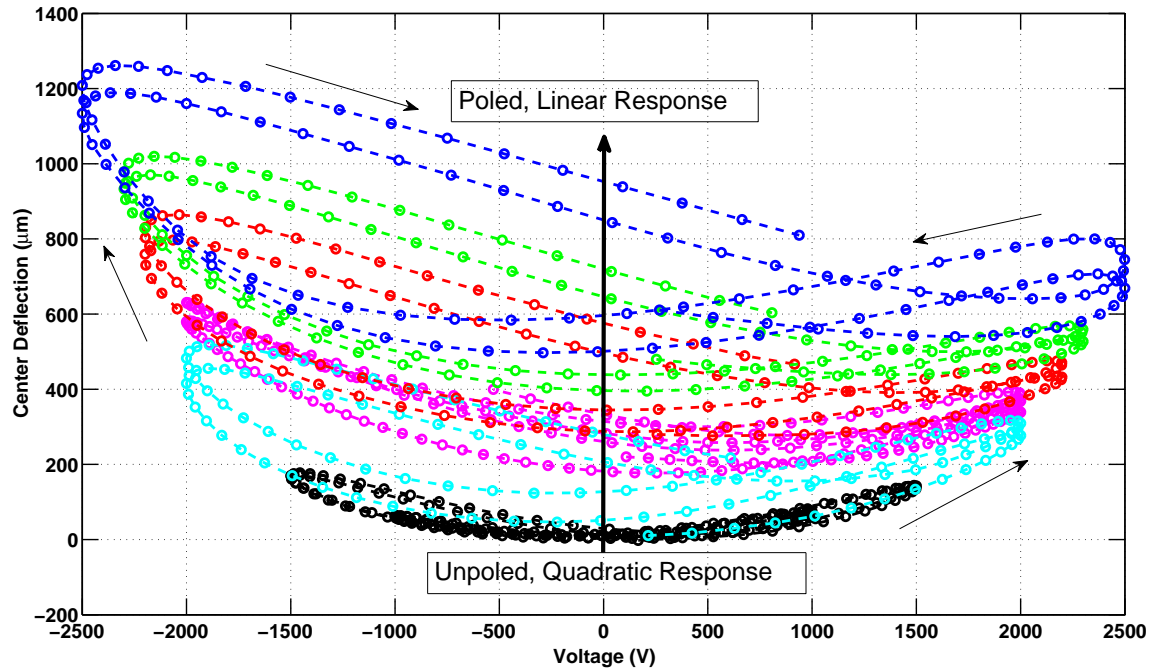


Figure 12. Single-actuator sample subjected to cycles of increasing voltage until the material is poled with a residual linear response.

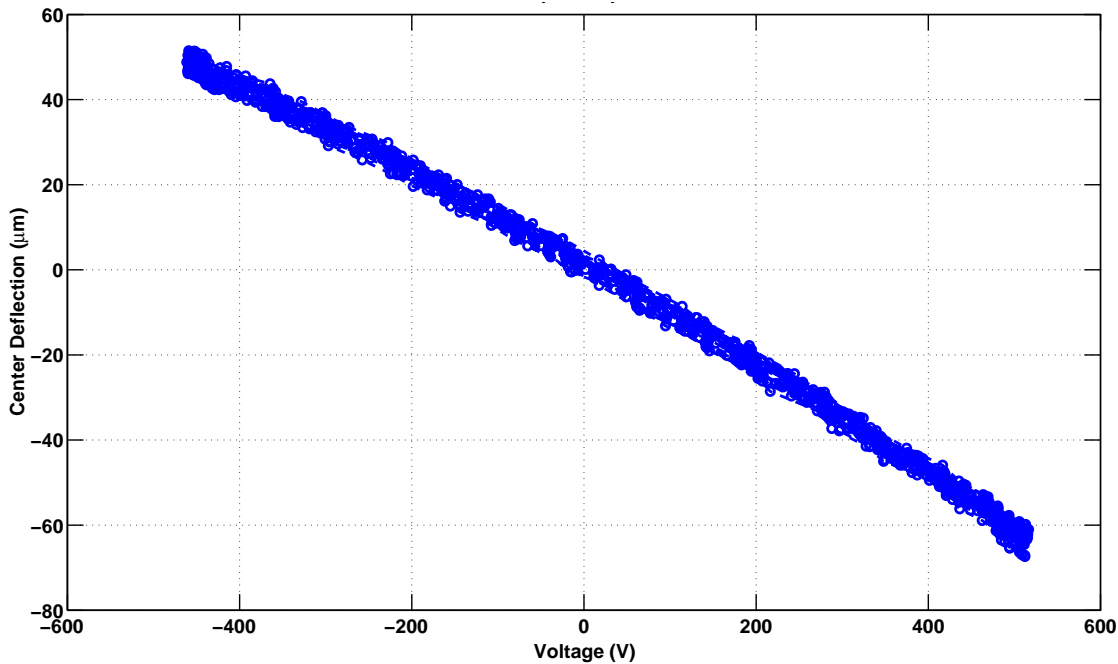


Figure 13. Deflection of the center point of a single-actuator mirror sample after poling of the material subject to 10 cycles of -500 to 500 volts. The observed behavior is indicative of a strong, nearly linear piezoelectric response with low hysteresis in the operating voltage range. The measurement error is on the order of 5 to 10 microns.

Acknowledgments

We thank Eleftherios Gdoutos for establishing the early fabrication effort, and Dr. Harish Manohara (JPL) for providing access to JPL Microdevices Lab (MDL) cleanroom facilities for sample fabrication. We also thank Drs. Risaku Toda and Victor White (JPL) for assistance and advice on sample fabrication. The students in the Caltech Ae105 class contributed greatly to the mission telescope concept design, and we would like to acknowledge their efforts here. We also thank Dr. Jim Breckinridge for helpful discussions on telescope design, John Steeves, Prof. Chiara Daraio (Caltech), and Dr. Andrew Shapiro (JPL) also for help and advice regarding the fabrication of prototype mirrors. We also appreciate the fabrication facilities provided by the Molecular Materials Research Center and Kavli Nanoscience Institute at Caltech. Financial support from the Keck Institute of Space Studies (KISS) at Caltech is gratefully acknowledged.

References

- ¹Breckinridge, J.B., Dooley, J., Ortiz, M. and Pellegrino, S., *Large Space Apertures (LSA) Study Report*, Keck Institute of Space Studies (2009).
- ²Katz, J.G. *Estimation and Control of Flexible Space Structures for Autonomous On-Orbit Assembly*, M.Sc. thesis in Aeronautics and Astronautics, MIT (2009).
- ³Natori, M.C., Ukegawa, K., "Concept of self-assembly of space structure systems using autonomous modules," *54th International Astronautical Congress of the International Astronautical Federation*, 29 September - 3 October 2003, Bremen, Germany, IAC-03-U.1.01 (2003).
- ⁴Wokes, D., Smail, S., Palmer, P., Underwood, C., "Pose estimation for in-orbit self-assembly of the intelligent self-powered modules," *AIAA Guidance, Navigation, and Control Conference* 10 - 13 August 2009, Chicago IL, AIAA 2009-6291 (2009)
- ⁵Rodgers, L.P. *Concepts and Technology Development for the Autonomous Assembly and Reconfiguration of Modular Space Systems*, M.Sc. thesis in Mechanical Engineering, MIT (2005).
- ⁶Hickey, G., Barbee, T., Ealey M., and Redding, D. "Actuated hybrid mirrors for space telescopes," *SPIE Astronomical Telescopes and Instrumentation* 7731-71 (2010).
- ⁷Romeo, R.C., Meinel, A.B., Meinel, M.P. and Chen, P.C., "Ultra-lightweight and hyper-thin rollable primary mirror for space telescopes," in *UV, Optical, and IR Space Telescopes and Instruments*, Breckinridge, J.B., ed., vol. 4013. SPIE, pp. 634-639 (2000).
- ⁸Lindler, J. and Flint, E., "Robustness of thin film shells with discrete boundary actuation," *47th AIAA/ASME/ASCE/AHS/ASC Structures, Structural Dynamics, and Materials Conference* (2006).
- ⁹de Blonk, B., Moore, J., Patrick, B., and Flint, E., "Membrane mirrors in space telescopes," in *Recent Advances in Gossamer Spacecraft*, Jenkins, C., ed., 45-108, American Institute of Aeronautics and Astronautics, Inc., Reston, Virginia (2006).
- ¹⁰Kuo, C.P., "A deformable mirror concept for adaptive optics in space," *SPIE Vol. 1542 Active/Adaptive Optical Systems* SPIE Vol. 1542 (1991).
- ¹¹Rodrigues, G., Bastait, R., Roose, S., Stockman, Y., Gebhardt, S., Schoenecker, A., Villon, P., and Preumont, A., "Modular bimorph mirrors for adaptive optics," in [*Optical Engineering*], Volume 48, Issue 3, pp. 034001-034001-7 (2009).
- ¹²Chen, Q., Natale, D., Neese, B., et al, "Piezoelectric polymers actuators for precise shape control of large scale space antennas," *SPIE Smart Structures and Materials and Nondestructive Evaluation and Health Monitoring* 07-0607 (2007).
- ¹³Sober, D.M. Jr., Agnes, G. S., Mollenhauer, D., "Smart structures for the control of optical surfaces," *44th AIAA/ASME/ASCE/AHS Structures, Structural Dynamics, and Materials Conference* AIAA 2003-1559 (2003).
- ¹⁴Pearson, J., Moore, J., and Fang, H., "Large and high precision inflatable membrane reflector," *51st AIAA/ASME/ASCE/AHS/ASC Structures, Structural Dynamics, and Materials Conference*, AIAA, Orlando, Florida (2010).
- ¹⁵Pearson, D.D., Cavaco, J.L., Roche, J., "Multichannel, surface parallel, zonal transducer system", U.S. Patent No. 7,683,524 B2. Washington, DC: U.S. Patent and Trademark Office (2010).
- ¹⁶Patterson, K., Pellegrino, S., and Breckinridge, J., "Shape correction of thin mirrors in a reconfigurable modular space telescope," *SPIE Astronomical Telescopes and Instrumentation* 7731-72 (2010).
- ¹⁷Patterson, K., and Pellegrino, S., "Shape Correction of Thin Mirrors," *52nd AIAA Structures, Structural Dynamics, and Materials Conference* AIAA-2011-1827 (2011).
- ¹⁸Bely, P., *The Design and Construction of Large Optical Telescopes*, Springer, New York (2003).
- ¹⁹Klein, R., *Concrete and Abstract Voronoi Diagrams*, Springer-Verlag, Berlin (1987).
- ²⁰Born, M., Wolf, E., *Principles of Optics*, Pergamon Press, Oxford (1989).
- ²¹Song, H., Simonov, A., Vdovin, G., "Multiplexing Control of a Multichannel Piezoelectric Deformable Mirror," *5th International Workshop on Adaptive Optics for Industry and Medicine* SPIE Vol. 6018 60181F-1 (2005).
- ²²Dargaville, T., et al., "Characterization, Performance and Optimization of PVDF as a Piezoelectric Film for Advanced Space Mirror Concepts," Sandia National Laboratories Report, SAND2005-6846 (2005).